Molecular Crystals and Liquid Crystals

ISSN: 1542-1406 (Print) 1563-5287 (Online) Journal homepage: http://www.tandfonline.com/loi/gmcl20

An ADE-FDTD Formulation for the Study of Liquid-Crystal Components in the Terahertz Spectrum

D. C. Zografopoulos, K. P. Prokopidis, S. Tofani, O. Chojnowska, R. Dąbrowski, E. E. Kriezis & R. Beccherelli

To cite this article: D. C. Zografopoulos, K. P. Prokopidis, S. Tofani, O. Chojnowska, R. Dąbrowski, E. E. Kriezis & R. Beccherelli (2015) An ADE-FDTD Formulation for the Study of Liquid-Crystal Components in the Terahertz Spectrum, Molecular Crystals and Liquid Crystals, 619:1, 49-60, DOI: 10.1080/15421406.2015.1087282

To link to this article: http://dx.doi.org/10.1080/15421406.2015.1087282

Mol. Cryst. Liq. Cryst., Vol. 619: pp. 49–60, 2015

ISSN: 1542-1406 print/1563-5287 online
DOI: 10.1080/15421406.2015.1087282

An ADE-FDTD Formulation for the Study of Liquid-Crystal Components in the Terahertz Spectrum

D. C. ZOGRAFOPOULOS,[1,*] K. P. PROKOPIDIS,[2] S. TOFANI,[1] O. CHOJNOWSKA,[3] R. DĄBROWSKI,[3] E. E. KRIEZIS,[2] AND R. BECCHERELLI[1]

[1]Consiglio Nazionale delle Ricerche, Istituto per la Microelettronica e Microsistemi (CNR-IMM), Rome, Italy
[2]Department of Electrical and Computer Engineering, Aristotle University of Thessaloniki, Thessaloniki, Greece
[3]Institute of Chemistry, Military University of Technology, Warsaw, Poland

An anisotropic auxiliary differential equation finite-difference time-domain formulation is presented in detail for the time-domain study of nematic liquid crystal devices in the terahertz spectrum. The termination of the computation domain is achieved by employing a properly designed convolution perfectly matched layer. The material dispersion and dichroism of the LC complex permittivities is modeled via a modified Lorentzian function that is demonstrated to provide an accurate description for a series of state-of-the-art materials used in LC-THz technology.

Keywords Finite-difference time-domain (FDTD) method; auxiliary differential equations; perfectly matched layer; anisotropic media; dispersive media; liquid crystals; terahertz technology.

Introduction

Nematic liquid crystals (LCs) are inherently anisotropic organic materials, whose properties can be dynamically controlled via the application of external control signals. Owing to their tunability and large inherent anisotropy, LCs have been proven as excellent candidate materials in a broad range of reconfigurable devices spanning from displays and light projection systems to optical/plasmonic waveguides, filters, switches, and other integrated components [1-6]. Recently, their use has been extended into the rapidly growing field of terahertz technology, which investigates thus far unexplored possibilities for novel devices in security, imaging, chemical detection, and short-range communications. In several experimental demonstrations, LCs have been proposed as tunable elements, such as phase modulators, polarizers, filters, beam-steerers, absorbers, and metamaterials [7-10].

*Address correspondence to D. C. Zografopoulos, Consiglio Nazionale delle Ricerche, Istituto per la Microelettronica e Microsistemi (CNR-IMM), Rome 00133, Italy. E-mail: dimitrios.zografopoulos@artov.imm.cnr.it

Color versions of one or more of the figures in the article can be found online at www.tandfonline.com/gmcl.

The design and investigation of advanced LC-THz components demands the availability of numerical tools, capable of accurately and efficiently describing the physics of electromagnetic (EM) wave interaction in anisotropic media. The finite-difference time-domain (FDTD) method is a classical tool for the fast and broadband analysis of EM components [11].

In FDTD studies, special care must be taken when the materials involved show significant dispersion of their properties inside the investigated spectrum. Several FDTD techniques have been already introduced for anisotropic media, both non-dispersive [12-15] and dispersive, such as plasma [16] and magnetized ferrites [17,18]. Material dispersion in FDTD can be taken into account by employing classical dispersion models, *e.g.* Drude or Lorentz, which have also been extended to particular cases involving anisotropic media [19]. However, the FDTD modeling of LC materials in the THz spectrum requires specific treatment, as these often exhibit strong material dispersion and dichroism, accompanied by appreciable amounts of absorption losses.

In this work, we present in detail an FDTD model based on the auxiliary differential equation formulation (ADE), which is suitable for the study of LC-THz components, as it takes rigorously into account both the LC anisotropy and the dispersion of their complex permittivities, the latter described by a modified Lorentzian (mLor) analytical function [20]. It is shown that the mLor model accurately describes the LC permittivity dispersion for a series of state-of-the-art LC materials specifically synthetized for THz applications. Moreover, the implementation of a convolution perfectly matched layer (CPML) for the efficient termination of the computational domain is also discussed. The proposed ADE-FDTD method constitutes a powerful numerical tool for the design and study of novel LC-tunable THz components.

Modified Lorentz Fitting of Liquid Crystal Permittivities

In the proposed formulation, both the ordinary and the extraordinary LC relative permittivities are described according to the modified Lorentzian dispersive model

$$\varepsilon_{o/e}(\omega) = \varepsilon_{\infty,o/e} + \frac{a_{1,o/e} j\omega + a_{0,o/e}}{b_{2,o/e}(j\omega)^2 + b_{1,o/e} j\omega + b_{0,o/e}}, \tag{1}$$

where a time dependence of $e^{j\omega t}$ is assumed. The mLor model has been recently proposed for the accurate description of material dispersion in time-domain studies [21] and it can be proved that it is encompasses other advanced models, namely the Drude critical points and the complex conjugate residual pairs, which have been developed for the FDTD modeling of highly dispersive materials, such as noble metals in the visible and infrared spectra [22-25]. In addition, it can be shown that Eq. (1) satisfies the Kramers-Kronig condition, thus providing a proper candidate for the description of the permittivity dispersion of real materials [26]. By setting $\alpha_1 = 0$, the mLor reduces to the well-known Lorentz model, which has been traditionally employed in FDTD studies. It is remarked, though, that adding the $a_1 j\omega$ term in the numerator of (1) does not imply additional memory and computational requirements in the proposed FDTD model, as it will be explained in Section 3.

Nematic liquid crystalline mixtures used in VIS/IR applications are typically characterized by refractive index dispersion described by the Cauchy model, while their absorption losses are negligible owing to the few-μm thickness of the employed cells. Thus, the real

Table 1. Fitted mLor parameters for the ordinary (o) and extraordinary (e) permittivities of a series of nematic liquid crystals proposed for THz technology applications

Ref.	LC	ε_∞	a_0	a_1 [ps]	b_0	b_1 [ps]	b_2 [ps^2]
[28]	5CB(o)	2	1.2622	0.2148	2.0746	0.5015	0.0041
	5CB(e)	2.4	3.3539	1.1795	6.1051	2.616	0.0156
[29]	BL037(o)	1.85	12.181	2.3726	14.6175	3.6541	0.03
	BL037(e)	2.272	1.7127	0.21	1.7621	0.2343	0
[30]	1855(o)	2.2	2.7662	0.3871	8.3725	1.5355	0
	1855(e)	2.5	9.5127	26.8743	0	77.921	0.3053
[31]	MixF(o)	2.299	0.3142	0.0597	2.728	1.0928	0.0559
	MixF(e)	3.441	0.9937	0	8.4694	0.849	0.0668
[31]	MixK(o)	2.276	0.0488	0.1216	0	1.5053	0.1989
	MixK(e)	2.68	0.0786	0.0103	3.3571	0.5495	0.0342
[31]	MixA(o)	2.35	0.3312	0	5.8977	0.6434	0.0521
	MixA(e)	2.859	0.6614	0	6.3508	0.6011	0.0575
[32]	1852(o)	2.357	0.1276	0.084	0.7739	0.9091	0.079
	1852(e)	3.45	0.696	0	5.5939	0.549	0.0388
[32]	1825(o)	2.3676	0.628	0	6.044	0.9635	0.0259
	1825(e)	3.6745	0.6355	0	4.8335	0.5127	0.0369

part of Eq. (1) is sufficient to accurately describe their dispersion in FDTD modeling [27]. However, when it comes to LC-THz technology where thicker LC cells are typically employed, nematic LCs usually exhibit strong dichroism and index dispersion, which does not follow any of the classical analytical models (LCs with small dichroism are also available [28]). In order to demonstrate the suitability of the mLor model, we have fitted experimentally measured data of the permittivities of a series of LC materials [28-32] by employing a nonlinear optimization Nelder-Mead technique [20]. The resulting mLor parameter coefficients are summarized in Table 1 and a direct comparison between the experimental data and the fitted functions is provided in Fig. 1. It can be observed that a single mLor term captures the dispersive behavior for both the real and imaginary permittivity parts, thus demonstrating the suitability of the proposed model for the time-domain modeling of LC-THz devices. Furthermore, we stress that apart from the accurate modeling of LCs, the mLor model in the proposed FDTD formulation can also naturally describe the dispersion of isotropic materials, e.g. metals, which is essential in problems such as the study of THz metamaterial devices with advanced functionalities [8-10].

Finite-difference Time-domain Formulation of Dispersive and Lossy Liquid Crystals

The relative permittivity tensor of a LC can be described by the general form

$$\tilde{\varepsilon} = \begin{pmatrix} \varepsilon_o + \Delta\varepsilon \cos^2\theta \cos^2\phi & \Delta\varepsilon \cos^2\theta \sin\phi \cos\phi & \Delta\varepsilon \sin\theta \cos\theta \cos\phi \\ \Delta\varepsilon \cos^2\theta \sin\phi \cos\phi & \varepsilon_o + \Delta\varepsilon \cos^2\theta \sin^2\phi & \Delta\varepsilon \sin\theta \cos\theta \sin\phi \\ \Delta\varepsilon \sin\theta \cos\theta \cos\phi & \Delta\varepsilon \sin\theta \cos\theta \sin\phi & \varepsilon_o + \Delta\varepsilon \sin^2\theta \end{pmatrix} \quad (2)$$

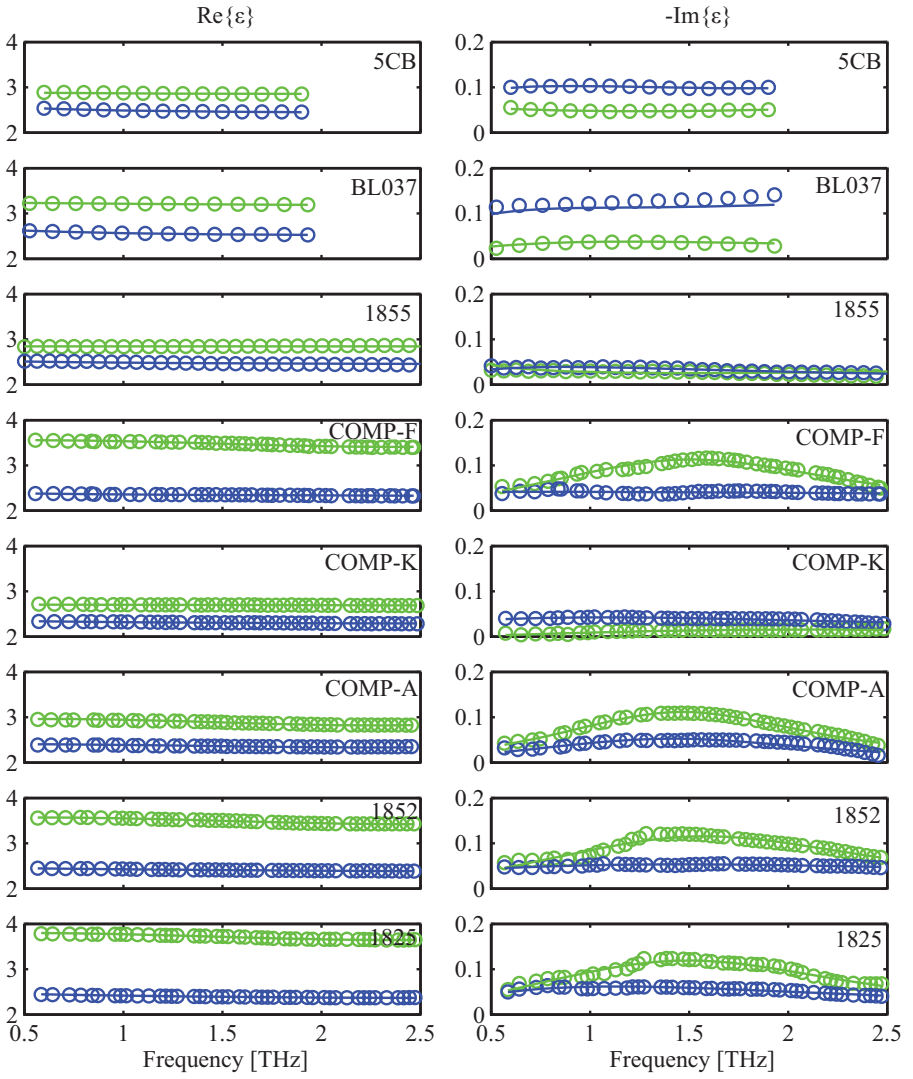

Figure 1. Comparison between the experimentally measured data (circles) of LC ordinary (blue) and extraordinary (green) permittivities and their fitting to the analytic mLor model (lines), for the coefficients reported in Table 1.

where θ and ϕ are the tilt and twist angles, respectively, according to Fig. 2(b), ε_o and ε_e are the ordinary and extraordinary dielectric constants with $\Delta\varepsilon = \varepsilon_e - \varepsilon_o$. An accurate description of liquid crystals would demand ε_o, ε_e to be functions of the electromagnetic wave frequency and as a result the permittivity tensor of (2) should account for this type of material dispersion. Such a medium can be termed as anisotropic-dispersive. If the imaginary parts of the ordinary and extraordinary permittivities are non-zero the medium exhibits losses, which in general can be different along the extraordinary and ordinary axes of the LC molecules (dichroism).

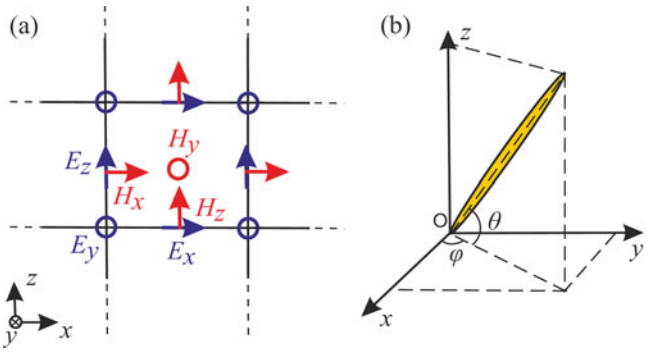

Figure 2. (a) The unit cell employed in the presented FDTD formulation, showing the positions of the electric and magnetic field components on the discretized grid. (b) The local LC orientation is described by the nematic director, defined via the spatially dependent tilt (θ) and twist (ϕ) angles.

We restrict ourselves to the case which the LC optical axis lies on a plane of the rectangular coordinate system and without loss of generality we assume that $\phi = 0$, and the LC optical axis lies on the $x - z$ plane. The permittivity tensor for this case is given by

$$\tilde{\varepsilon} = \begin{pmatrix} \varepsilon_o + \Delta\varepsilon \cos^2\theta & 0 & \Delta\varepsilon \sin\theta \cos\theta \\ 0 & \varepsilon_o & 0 \\ \Delta\varepsilon \sin\theta \cos\theta & 0 & \varepsilon_o + \Delta\varepsilon \sin^2\theta \end{pmatrix}, \tag{3}$$

where it is stressed that the parameters ε_o, $\Delta\varepsilon$ are frequency-dependent. The constitutive relation of the medium in the frequency domain is expressed as

$$\mathbf{D}(\omega) = \varepsilon_0 \tilde{\varepsilon}(\omega)\mathbf{E}(\omega), \tag{4}$$

where ε_0 is the permittivity of free space. The components of the electric flux density are

$$D_x = \varepsilon_0[\varepsilon_o(\omega) + \Delta\varepsilon(\omega)\cos^2\theta]E_x + \varepsilon_0\Delta\varepsilon(\omega)\sin\theta\cos\theta E_z \tag{5}$$

$$D_y = \varepsilon_0\varepsilon_o(\omega)E_y \tag{6}$$

$$D_z = \varepsilon_0\Delta\varepsilon(\omega)\sin\theta\cos\theta E_x + \varepsilon_0[\varepsilon_o(\omega) + \Delta\varepsilon(\omega)\sin^2\theta]E_z \tag{7}$$

It is observed that (6) is similar to the constitutive relation of an isotropic medium, but (5) and (7) involve both x- and z-components of the electric field and should be solved simultaneously. We now introduce auxiliary variables in order to split the x- and z-components of the electric field. Equations (5) and (7) are written as

$$D_x = P_{x1} + P_{x2} + P_{z1} + P_{z2} \tag{8}$$

$$D_z = Q_{x1} + Q_{x2} + Q_{z1} + Q_{z2}, \tag{9}$$

with the auxiliary variables defined as

$$P_{x1} = \varepsilon_0\varepsilon_o(\omega)\sin^2\theta E_x, \quad P_{x2} = \varepsilon_0\varepsilon_e(\omega)\cos^2\theta E_x \tag{10}$$

$$P_{z1} = \varepsilon_0\varepsilon_e(\omega)\sin\theta\cos\theta E_z, \quad P_{z2} = -\varepsilon_0\varepsilon_o(\omega)\sin\theta\cos\theta E_z, \tag{11}$$

and

$$Q_{x1} = \varepsilon_0 \varepsilon_e(\omega) \sin\theta \cos\theta E_x, \quad Q_{x2} = -\varepsilon_0 \varepsilon_o(\omega) \sin\theta \cos\theta E_x \tag{12}$$

$$Q_{z1} = \varepsilon_0 \varepsilon_o(\omega) \cos^2\theta E_z, \quad Q_{z2} = \varepsilon_0 \varepsilon_e(\omega) \sin^2\theta E_z. \tag{13}$$

In the following, we assume that $\varepsilon_o(\omega)$ and $\varepsilon_e(\omega)$ follow the modified Lorentz dispersion model of (1) and the parameters are obtained through the fitting procedure presented in the previous Section. In the above expressions the angle θ is not function of frequency, but it can be spatially dependent, i.e. in general it can be $\theta = \theta(x, z)$ for the case of inhomogeneous LC orientation profiles. From equations (10)-(13) the governing equations of the auxiliary variables can be obtained. For the case of the P_{x1}, the following differential equation is derived, which is similar in form to the isotropic case [24]

$$\left(b_{2,o}\frac{d^2}{dt^2} + b_{1,o}\frac{d}{dt} + b_{0,o}\right) P_{x1} = \varepsilon_0 \sin^2\theta \times \left[\varepsilon_{\infty,o} b_{2,o}\frac{d^2}{dt^2} + (a_{1,o} + \varepsilon_{\infty,o} b_{1,o})\frac{d}{dt} + (a_{0,o} + \varepsilon_{\infty,o} b_{0,o})\right] E_x. \tag{14}$$

Up to this point no numerical discretization technique has been implied. In addition, no assumption of the relative position of the field components is made and therefore the scheme of spatial discretization used in the following can be staggered, unstaggered, collocated etc. As described in [24], we discretize the above differential equation in time using central averaging and difference operators and we get the following difference equation

$$\left(b_{2,o}\frac{\delta_t^2}{\Delta t^2} + b_{1,o}\frac{\delta_t \mu_t}{\Delta t} + b_{0,o}\mu_t^2\right) P_{x1}^n = \varepsilon_0 \sin^2\theta \left[\varepsilon_{\infty,o} b_{2,o}\frac{\delta_t^2}{\Delta t^2} + (a_{1,o} + b_{1,o}\varepsilon_{\infty,o})\frac{\delta_t \mu_t}{\Delta t} + (a_{0,o} + b_{0,o}\varepsilon_{\infty,o})\mu_t^2\right] E_x^n \tag{15}$$

where Δt is the time step of the FDTD method and the operators δ_t and μ_t are defined as follows

$$\delta_t f^n = f^{n+1/2} - f^{n-1/2}, \; \mu_t f^n = \tfrac{1}{2}\left(f^{n+1/2} + f^{n+1/2}\right). \tag{16}$$

The update equation for the variable P_{x1} is

$$P_{x1}^{n+1} = \frac{1}{c_{o1}}\left(c_{o4}\varepsilon_0 \sin^2\theta E_x^{n+1} + c_{o5}\varepsilon_0 \sin^2\theta E_x^n + c_{o6}\varepsilon_0 \sin^2\theta E_x^{n-1} - c_{o2}P_{x1}^n - c_{o3}P_{x1}^{n-1}\right) \tag{17}$$

with

$$c_{o1} = \frac{b_{2,o}}{\Delta t^2} + \frac{b_{1,o}}{2\Delta t} + \frac{b_{0,o}}{4}, \; c_{o2} = -\frac{2b_{2,o}}{\Delta t^2} + \frac{b_{0,o}}{2}, \; c_{o3} = \frac{b_{2,o}}{\Delta t^2} - \frac{b_{1,o}}{2\Delta t} + \frac{b_{0,o}}{4} \tag{18}$$

$$c_{o4} = \frac{\varepsilon_{\infty,o} b_{2,o}}{\Delta t^2} + \frac{a_{1,o} + \varepsilon_{\infty,o} b_{1,o}}{2\Delta t} + \frac{a_{0,o} + \varepsilon_{\infty,o} b_{0,o}}{4},$$

$$c_{o5} = -\frac{2\varepsilon_{\infty,o} b_{2,o}}{\Delta t^2} + \frac{a_{0,o} + \varepsilon_{\infty,o} b_{0,o}}{2},$$

$$c_{o,6} = \frac{\varepsilon_{\infty,o} b_{2,o}}{\Delta t^2} - \frac{a_{1,o} + \varepsilon_{\infty,o} b_{1,o}}{2\Delta t} + \frac{a_{0,o} + \varepsilon_{\infty,o} b_{0,o}}{4} \tag{19}$$

Similar update equations are obtained for the other auxiliary variables. Equations (8) and (9) are taken at time $(n+1)\Delta t$ as

$$D_x^{n+1} = P_{x1}^{n+1} + P_{x2}^{n+1} + P_{z1}^{n+1} + P_{z2}^{n+1} \tag{20}$$

$$D_z^{n+1} = Q_{x1}^{n+1} + Q_{x2}^{n+1} + Q_{z1}^{n+1} + Q_{z2}^{n+1}. \tag{21}$$

After substitution of the auxiliary variables the following linear 2×2 system is formed with respect to E_x^{n+1} and E_z^{n+1}

$$\begin{aligned} a_{x1}E_x^{n+1} + a_{z1}E_z^{n+1} &= A \\ b_{x1}E_x^{n+1} + b_{z1}E_z^{n+1} &= B \end{aligned} \tag{22}$$

with

$$\begin{aligned} A = {} & D_x^{n+1} - a_{x2}E_x^n - a_{x3}E_x^{n-1} - a_{x4}P_{x1}^n - a_{x5}P_{x2}^n - a_{x6}P_{x1}^{n-1} - a_{x7}P_{x2}^{n-1} \\ & - a_{z2}E_z^n - a_{z3}E_z^{n-1} - a_{z4}P_{z1}^n - a_{z5}P_{z2}^n - a_{z6}P_{z1}^{n-1} - a_{z7}P_{z2}^{n-1} \end{aligned} \tag{23}$$

$$\begin{aligned} B = {} & D_z^{n+1} - b_{x2}E_x^n - b_{x3}E_x^{n-1} - b_{x4}Q_{x1}^n - b_{x5}Q_{x2}^n - b_{x6}Q_{x1}^{n-1} - b_{x7}Q_{x2}^{n-1} \\ & - b_{z2}E_z^n - b_{z3}E_z^{n-1} - b_{z4}Q_{z1}^n - b_{z5}Q_{z2}^n - b_{z6}Q_{z1}^{n-1} - b_{z7}Q_{z2}^{n-1}, \end{aligned} \tag{24}$$

where the corresponding coefficients are defined as

$$a_{x1} = \frac{\varepsilon_0 c_{o4}\sin^2\theta}{c_{o1}} + \frac{\varepsilon_0 c_{e4}\cos^2\theta}{c_{e1}},\ a_{x2} = \frac{\varepsilon_0 c_{o5}\sin^2\theta}{c_{o1}} + \frac{\varepsilon_0 c_{e5}\cos^2\theta}{c_{e1}},$$

$$a_{x3} = \frac{\varepsilon_0 c_{o6}\sin^2\theta}{c_{o1}} + \frac{\varepsilon_0 c_{e6}\cos^2\theta}{c_{e1}}, \tag{25}$$

$$a_{x4} = -\frac{c_{o2}}{c_{o1}},\ a_{x5} = -\frac{c_{e2}}{c_{e1}},\ a_{x6} = -\frac{c_{o3}}{c_{o1}},\ a_{x7} = -\frac{c_{e3}}{c_{e1}} \tag{26}$$

$$a_{z1} = \frac{\varepsilon_0 c_{e4}\sin\theta\cos\theta}{c_{e1}} - \frac{\varepsilon_0 c_{o4}\sin\theta\cos\theta}{c_{o1}},\ a_{z2} = \frac{\varepsilon_0 c_{e5}\sin\theta\cos\theta}{c_{e1}} - \frac{\varepsilon_0 c_{o5}\sin\theta\cos\theta}{c_{o1}},$$

$$a_{z3} = \frac{\varepsilon_0 c_{e6}\sin\theta\cos\theta}{c_{e1}} - \frac{\varepsilon_0 c_{o6}\sin\theta\cos\theta}{c_{o1}}, \tag{27}$$

$$a_{z4} = -\frac{c_{e2}}{c_{e1}},\ a_{z5} = -\frac{c_{o2}}{c_{o1}},\ a_{z6} = -\frac{c_{e3}}{c_{e1}},\ a_{z7} = -\frac{c_{o3}}{c_{o1}} \tag{28}$$

and

$$b_{x1} = a_{z1},\ b_{x2} = a_{z2},\ b_{x3} = a_{z3},\ b_{x4} = a_{z4},\ b_{x5} = a_{z5},\ b_{x6} = a_{z6},\ b_{x7} = a_{z7} \tag{29}$$

$$b_{z1} = \frac{\varepsilon_0 c_{o4}\cos^2\theta}{c_{o1}} + \frac{\varepsilon_0 c_{e4}\sin^2\theta}{c_{e1}},\ b_{z2} = \frac{\varepsilon_0 c_{o5}\cos^2\theta}{c_{o1}} + \frac{\varepsilon_0 c_{e5}\sin^2\theta}{c_{e1}},$$

$$b_{z3} = \frac{\varepsilon_0 c_{o6}\cos^2\theta}{c_{o1}} + \frac{\varepsilon_0 c_{e6}\sin^2\theta}{c_{e1}} \tag{30}$$

$$b_{z4} = -\frac{c_{o2}}{c_{o1}},\ b_{z5} = -\frac{c_{e2}}{c_{e1}},\ b_{z6} = -\frac{c_{o3}}{c_{o1}},\ b_{z7} = -\frac{c_{e3}}{c_{e1}}. \tag{31}$$

Since A and B contain already calculated values of previous time steps, E_x and E_z are updated after solving the linear system

$$E_x^{n+1} = \frac{Ab_{z1} - Ba_{z1}}{a_{x1}b_{z1} - a_{z1}b_{x1}},\ E_z^{n+1} = \frac{Ba_{x1} - Ab_{x1}}{a_{x1}b_{z1} - a_{z1}b_{x1}} \tag{32}$$

The fields D_x^{n+1} and D_z^{n+1} are obtained through the implementation of Faraday's law, i.e.

$$D_x^{n+1}(i+\tfrac{1}{2},k) = D_x^n(i+\tfrac{1}{2},k) - \frac{\Delta t}{\Delta z}\left(H_y^{n+1/2}\left(i+\tfrac{1}{2},k+\tfrac{1}{2}\right)\right.$$
$$\left. - H_y^{n+1/2}(i+\tfrac{1}{2},k-\tfrac{1}{2})\right) \tag{33}$$

$$D_z^{n+1}(i,k+\tfrac{1}{2}) = D_z^n(i,k+\tfrac{1}{2}) + \frac{\Delta t}{\Delta x}\left(H_y^{n+1/2}\left(i+\tfrac{1}{2},k+\tfrac{1}{2}\right)\right.$$
$$\left. - H_y^{n+1/2}(i-\tfrac{1}{2},k+\tfrac{1}{2})\right). \tag{34}$$

An important issue in modeling anisotropic media with the FDTD method is that the electric components are staggered in space and they are located in different positions in the FDTD grid, as shown in Fig 1(a). Therefore, it is necessary to employ the averaging of field values located at the surrounding nodes. In particular, for the update of x-component in Eq. (32), the parameter A involves the fields E_z, P_{z1}, P_{z2} while B the values of E_z, Q_{z1}, Q_{z2}, which are defined in different positions compared to the x- component. It is also noted that for inhomogeneous media the variable θ can be a function of space $\theta = \theta(i,k)$, where the integers i, k are the indices in the FDTD grid i.e. $x = i\Delta x$ and $z = k\Delta z$. Since the location of the x-component of the electric field is $(i+1/2, k)$, the angle θ should be defined in the same position. A different case applies to Eq. (7), where θ should be defined at $(i, k+1/2)$.

It has been proved in [33] that improper averaging in inhomogeneous anisotropic media may lead to instability problems and a stable algorithm has been proposed there for non-dispersive tensors, which is symmetric and positive semi-definite. The non-reciprocity of the simple averaging, which may potentially lead instability, has also been discussed in [34]. In [33], it is stated that simulations with absorbing boundary conditions and/or significant dissipation are insensitive to such instabilities. Since we will deal with dispersive-anisotropic media, the simple averaging procedure will be used, i.e.

$$E_z(i+\tfrac{1}{2},k) \simeq \tfrac{1}{4}\left(E_z(i,k+\tfrac{1}{2}) + E_z(i,k-\tfrac{1}{2}) + E_z(i+1,k+\tfrac{1}{2}) + E_z(i+1,k-\tfrac{1}{2})\right). \tag{35}$$

Assuming that the x-component of the electric field is calculated first, it is remarked that for the update of the z-component of the electric field the value of the x-component electric field of time step n and $n-1$ is needed and not the value of the current step E_x^{n+1}. As a result, three previous values should be kept in memory. On the contrary, in the calculation of E_x^{n+1} two previous time steps are necessary.

Convolution Perfectly Matched Layer as an Absorbing Boundary Condition to Terminate Domains with Anisotropic-lossy Liquid Crystals

In FDTD simulations, it is necessary to terminate the computational domain with an absorbing boundary condition (ABC), which absorbs the outgoing waves and mitigates an "infinite" domain [11]. Among ABCs, the Perfectly Matched Layer (PML) is the most successful and efficient method and it is widely used in computational electromagnetics.

Several PML formulations have been proposed in order to overcome the limitations of the original technique proposed by Bérenger [11]. The Convolution PML (CPML) [35] offers a number of advantages over other PML methods including the ability to absorb evanescent waves, significant memory savings and independence of the host medium.

In the present work, we apply the CPML theory to anisotropic-dispersive media described by the tensor given by (3). Our ADE-based formulation allows for seamless combination with CPML and it can be efficiently incorporated in existing CPML-FDTD codes. Assuming the same two-dimensional FDTD domain ($x-z$ plane) as previously, Maxwell's equations inside the CPML have the form

$$j\omega D_x = -\frac{1}{s_z}\frac{\partial H_y}{\partial z},\ j\omega D_y = \frac{1}{s_z}\frac{\partial H_x}{\partial z} - \frac{1}{s_x}\frac{\partial H_z}{\partial x},\ j\omega D_z = \frac{1}{s_x}\frac{\partial H_y}{\partial x} \tag{36}$$

$$j\omega\mu_0 H_x = \frac{1}{s_z^*}\frac{\partial E_y}{\partial z},\ j\omega\mu_0 H_y = -\frac{1}{s_z^*}\frac{\partial E_x}{\partial z} + \frac{1}{s_x^*}\frac{\partial E_z}{\partial x},\ j\omega\mu_0 H_z = -\frac{1}{s_x^*}\frac{\partial E_y}{\partial x} \tag{37}$$

where s_η, $\eta = x, z$ is the stretched-coordinate metric defined as

$$s_\eta = \kappa_\eta + \frac{\sigma_\eta}{\alpha_\eta + j\omega\varepsilon_0}, \tag{38}$$

with parameters defined as in [35]. By transferring (36), (37) into the time domain we obtain the following update equations

$$\frac{\partial D_x}{\partial t} = -\frac{1}{\kappa_z}\frac{\partial H_y}{\partial z} - \psi_{exz} \tag{39}$$

$$\frac{\partial D_y}{\partial t} = \frac{1}{\kappa_z}\frac{\partial H_x}{\partial z} - \frac{1}{\kappa_x}\frac{\partial H_z}{\partial x} + \psi_{eyz} - \psi_{eyx} \tag{40}$$

$$\frac{\partial D_z}{\partial t} = \frac{1}{\kappa_x}\frac{\partial H_y}{\partial x} + \psi_{ezx} \tag{41}$$

$$\mu_0\frac{\partial H_x}{\partial t} = \frac{1}{\kappa_z}\frac{\partial E_y}{\partial z} + \psi_{hxz} \tag{42}$$

$$\mu_0\frac{\partial H_y}{\partial t} = -\frac{1}{\kappa_z}\frac{\partial E_x}{\partial z} + \frac{1}{\kappa_x}\frac{\partial E_z}{\partial x} - \psi_{hyz} + \psi_{hyx} \tag{43}$$

$$\mu_0\frac{\partial H_z}{\partial t} = -\frac{1}{\kappa_x}\frac{\partial E_y}{\partial x} - \psi_{hzx} \tag{44}$$

According to the CPML formulation, the proposed algorithm for each step of the FDTD method is described as follows:

1. The auxiliary variables $\psi_{hxz}, \psi_{hyz}, \psi_{hyx}, \psi_{hzx}$ are updated as in the original CPML method [35].
2. The magnetic fields H_x, H_y, H_z are updated using (42), (43) and (44), respectively.
3. The auxiliary variables $\psi_{exz}, \psi_{eyz}, \psi_{eyx}, \psi_{exz}$ are updated as in the original CPML method.
4. The electric flux densities D_x, D_y, D_z are update using (39), (40) and (41), respectively.
5. The electric field E_x is updated using (32).

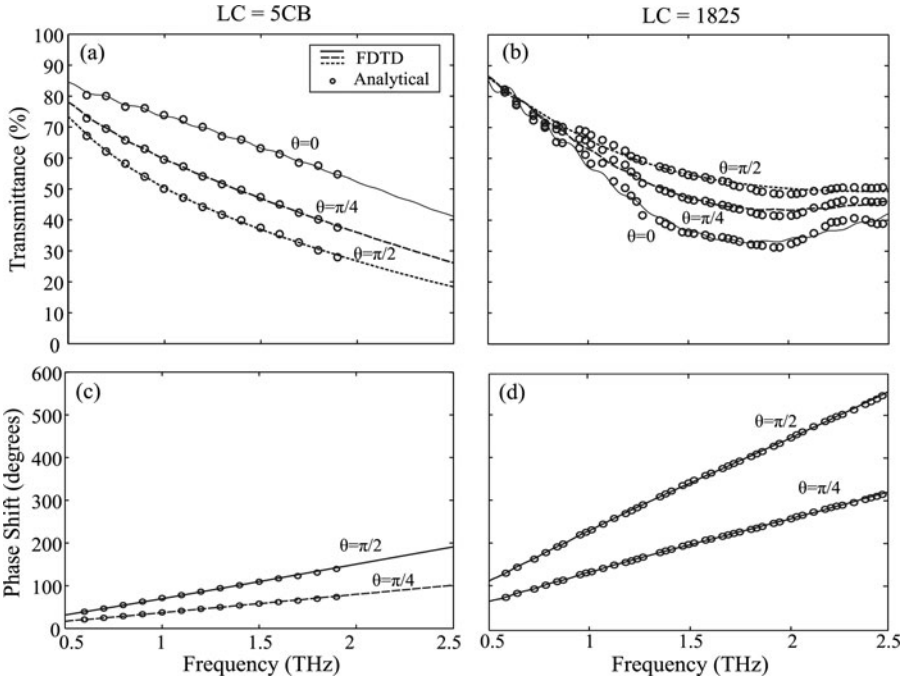

Figure 3. (a)-(b) Transmittance for different values of angle θ for the LC materials 5CB and 1825, respectively. (c)-(d) Phase shift with respect to the case $\theta = 0$ for 5CB and 1825, respectively. Circles correspond to the analytically calculated results based on measured data of LC permittivities at various frequencies.

6. The auxiliary variables P_{x1}, P_{x2}, Q_{x1}, Q_{x2} are updated with equations similar to (17).
7. The electric field E_y is updated as in an isotropic modified Lorentz medium.
8. The electric field E_z is updated using (32).
9. The auxiliary variables P_{z1}, P_{z2}, Q_{z1}, Q_{z2} are updated with equations similar to (17).

Numerical Results

The accuracy of the proposed fitting of the mLor functions and the efficiency of the introduced FDTD method are demonstrated in a benchmark problem of a LC slab embedded in a low-loss polymer with refractive index $n = 1.5$. An analytical solution is available for such a problem and a comparison with the proposed formulation is straightforward. The LC slabs have a thickness d $= 500\,\mu$m and the mLor parameters of the ordinary and extraordinary indexes are taken from Table 1 for two materials, the single-compound well-known nematic LC 5CB and the optimized high-Δn mixture 1825, which is specifically synthetized for THz applications. The EM wave is propagating toward the z-direction and impinges normally on the LC slab. The optical axis of the LC slab lies on the $x - z$ plane. The FDTD grid size is $\Delta z = 2\,\mu$m and a time step $\Delta t = Q\Delta z/c_0$ is employed, where $Q = 0.3$ and c_0 the velocity of light in vacuum. The computational domain is terminated by a 12-cell CPML and the wave is excited through the x-electric field component. A

modulated Gaussian pulse is used as excitation function with frequency content in the spectral region of interest (0.5-2.5 THz). The incident fields are calculated in the same computational domain without the slab.

The analytical solution is given by [36] taking into account the effective refractive index of the slab given by

$$n_{eff} = \frac{n_e n_o}{\sqrt{n_e^2 \sin^2\theta + n_o^2 \cos^2\theta}} \tag{45}$$

with the convention of θ as previously described. In Fig. 3, the transmittance and the reflectance are presented for the two test LC materials and three different values of angle θ. The calculated results are in very good agreement with respect to the analytical ones in the whole spectral region under study. Although 5CB and 1825 show similar losses, the mixture 1825 can provide larger phase-shift owing to the greater value of Δn. It is stressed that the numerical results are obtained with a single FDTD run, thus enabling the wideband modeling of LC-THz devices, which is a major advantage of the proposed formulation.

Conclusions

In brief, we have presented in detail a numerical framework based on the ADE-FDTD method for the time-domain simulation of electromagnetic field propagation in THz devices comprising nematic liquid crystalline materials. The LC anisotropy has been rigorously implemented and, furthermore, the dispersion of both real and imaginary parts of the LC permittivities has been accounted for, via its description with a modified Lorentzian function. The proposed method can provide a valuable tool in the design and investigation of LC-based tunable components for terahertz technology.

Acknowledgments

This work was supported by the Italian Ministry of Foreign Affairs, Directorate General for the Country Promotion, and by the projects PBS 847.

References

[1] Zografopoulos, D. C., Asquini, R., Kriezis, E. E., d'Alessandro, A., & Beccherelli, R. (2012). *Lab Chip*, *12*, 3598.
[2] Zografopoulos, D. C. & Beccherelli, R. (2013). *Appl. Phys. Lett.*, *102*, 101103.
[3] Zografopoulos, D. C. & Beccherelli, R. (2013). *Opt. Express*, *21*, 8240.
[4] Zografopoulos, D. C. & Beccherelli, R. (2013). *J. Opt.*, *15*, 055009.
[5] Zografopoulos, D. C. & Beccherelli, R. (2013). *Plasmonics*, *8*, 599.
[6] Zografopoulos, D. C., Beccherelli, R., Tasolamprou, A., & Kriezis, E. E. (2013). *Photonics Nanosctruct.Fundam. Appl.*, *11*, 73.
[7] Vieweg, N., Jansen, C., & Koch, M. (2013). "Liquid crystals and their applications in the THz frequency range," in *Terahertz spectroscopy and imaging*, vol. 171 of Springer Series in Optical Sciences, K.-E. Peiponen, A. Zeitler, and M. Kuwata-Gonokami, eds. (Springer, 2013), pp. 301–326.
[8] Chang, C.-L., Wang, W.-C., Lin, H.-R., Hsieh, F. J., Pun, Y.-B., & Chan, C.-H. (2013). *Appl. Phys. Lett.*, *102*, 151903.
[9] Shrekenhamer, D., Chen, W.-C., & Padilla, W. J. (2013). *Phys. Rev. Lett.*, *110*, 177403.
[10] Isić, G., Vasić, B., Zografopoulos, D. C., Beccherelli, R., & Gajić, R. (2015). *Phys. Rev. Applied*, *3*, 064007.

[11] Taflove, A. (2005). *Computational Electrodynamics: The Finite-Difference Time-Domain Method*, Artech House: Boston, MA.
[12] Schneider, J. & Hudson, S. (1993). *IEEE Trans. Antennas Propag.*, *41*, 994.
[13] Garcia, S. G., Hung-Bao, T. M., Martin R. G. & Olmedo, B. G. (1996). *IEEE Trans. Microwave Theory Tech.*, *44*, 2195.
[14] Zhao, A. P., Juntunen, J. & Raisanen, A. V. (1999). *IEEE Trans. Microwave Theory Tech.*, *47*, 1142.
[15] Duo, L. & Sebak, A. R. (2006). *Microwave Opt. Technol. Lett.*, *48*, 2083.
[16] Hunsberger, F., Luebbers, R. & Kunz, L. (1992). *IEEE Trans. Antennas Propag.*, *40*, 1489.
[17] Pereda, J. A., Vielva, L. A., Vegas, A. & Prieto, A. (1993) *IEEE Microw. Guided Wave Lett.*, *3*, 136.
[18] Grande, A., Pereda, J. A., Gonzales, O. & Vegas, A. (2009). *Int. J. Numer. Modeling: Electron. Netw., Devices Fields*, *22*, 109.
[19] Mosallaei, H. (2007) *IEEE Trans. Electromagn. Compat.*, *49*, 649.
[20] Zografopoulos, D. C., Prokopidis, K. P., Dąbrowski, R. & Beccherelli, R. (2014) *Opt. Mat. Exp.*, *4*, 449.
[21] Deinega, A. & John, S. (2012). *Opt. Lett.*, *37*, 112.
[22] Prokopidis, K. P. & Zografopoulos, D. C. (2013). *J. Lightwave Technol.*, *31*, 2467.
[23] Prokopidis, K. P. & Zografopoulos, D. C. (2013). *Electron. Lett.*, *49*, 534.
[24] Prokopidis, K. P & Zografopoulos, D. C. (2014). *IEEE Microw. and Wireless Compon. Lett.*, *24*, 659.
[25] Prokopidis, K. P. & Zografopoulos, D. C. (2014). *Photon. Technol. Lett.*, *26*, 2267.
[26] Prokopidis, K. & Kalialakis, C. (2014) *Appl. Phys. B*, *117*, 25.
[27] Prokopidis, K. P., Zografopoulos, D. C. & Kriezis, E. E. (2013). *J. Opt. Soc. Amer. B*, *30*, 2722.
[28] Reuter, M., Garbat, K., Vieweg, N., Fischer, B. M., Dąbrowski, R., Koch, M., Dziaduszek, J., & Urban, S. (2013). *J. Mater. Chem. C*, *1*, 4457.
[29] Vieweg, N., Shakfa, M. K., Scherger, B., Mikulics, M., & Koch, M. (2010). *J. Infrared Milli. Terahz. Waves*, *31*, 1312.
[30] Park, H., Parrott, E. P. J., Fan, F., Lim, M., Han, H., Chigrinov, V. G., & Pickell-MacPherson, P. (2012). *Opt. Express*, *4*, 449.
[31] Chodorow, U., Parka, J., & Chojnowska, O. (2012). *Photon. Lett. Poland*, *4*, 112.
[32] Reuter, M., Vieweg, N., Fischer, B. M., Mikulicz, M., Koch, M., Garbat, K., & Dąbrowski, R. (2013). *APL Mater.*, *1*, 012107.
[33] Werner G. R & Cary J. R. (2007). *J. Comput. Phys.*, *226*, 1085.
[34] Railton C. J. (2014). *IEEE Trans. Antennas Propag.*, *62*, 2688.
[35] Roden, J. A. & Gedney, S. D. (2000). *Microwave Opt. Technol. Lett.*, *27*, 334.
[36] Orfanidis, S. J. (2008). *Electromagnetic Waves and Antennas*, Rutgers University: Piscataway, NJ, (http://www.ece.rutgers.edu/∼orfanidi/ewa/)